Fermi National Accelerator Laboratory

FERMILAB-Conf-98/162-E
CDF and D0

Jet Production at the Tevatron

Freedy Nang
For the CDF and D0 Collaborations

Department of Physics, University of Arizona
Tucson, Arizona 85721

Fermi National Accelerator Laboratory
P.O. Box 500, Batavia, Illinois 60510

June 1998

Published Proceedings of the *Second Latin American Symposium on High Energy Physics*,
San Juan, Puerto Rico, April 8-11, 1998

Operated by Universities Research Association Inc. under Contract No. DE-AC02-76CH03000 with the United States Department of Energy

Disclaimer

Distribution

Jet Production at the Tevatron

Freedy Nang [1]

Department of Physics, University of Arizona, Tucson, AZ 85721

Abstract.

We present several results on high P_T jet production and compare them to the most recent theoretical predictions using the latest parton distribution functions. The dijet invariant mass distribution, triple differential cross section, and dijet angular distribution measurements exhibit very good agreement with the theoretical predictions. The latter agreement obviates the need to invoke compositeness models. At $\sqrt{s} = 630$ GeV , the inclusive jet cross section lies $15 - 20\%$ below the theoretical predictions for both experiments. At $\sqrt{s} = 1800$ GeV, the DØ inclusive jet cross section is in agreement with the theoretical predictions over the entire jet E_T range, the CDF collaboration observes an excess in the cross section for E_T above 200 GeV.

INTRODUCTION

Two years ago, the CDF collaboration generated great excitement when it published the inclusive jet cross section at $\sqrt{s} = 1800$ GeV showing an excess in the high transverse energy (E_T) region when compared to a next-to-leading order (NLO) theory [1]. The inclusive jet cross section measurement could deviate from the theory due to a variety of reasons, the most interesting of which is quark compositeness. Other explanations for the excess include the existence of new particles and differences between parton distribution functions (PDF's). We examine various results from both the CDF and DØ experiments, starting with the inclusive jet cross section at $\sqrt{s} = 1800$ GeV and 630 GeV. We also present results on the dijet angular distribution, the dijet invariant mass analysis and the triple differential dijet cross section.

THEORY

Perturbative QCD (pQCD) allows us to calculate any jet cross section as a convolution of the parton distribution functions for the incoming particles and the parton-parton hard scattering cross section:

---

[1] for the CDF and DØ Collaborations.

$$\sigma \sim \sum_{i,j} f_i(x_1, Q^2) f_j(x_2, Q^2) \hat{\sigma}_{ij} \ , \tag{1}$$

where $x_{1(2)}$ represents the momentum fraction of the proton (anti-proton) carried by the colliding parton; $f_{i,j}$ represent the parton distribution functions for the initial valence quarks (u, $\bar{u}$, d, $\bar{d}$) or sea partons (g, u, d, s, ...), evaluated at the energy scale of the hard scattering, Q^2; and $\hat{\sigma}_{ij}$ represents the cross section for the scattering of partons i and j. The relationship between the momentum fraction and pseudorapidity (η) is given by

$$x_{1,2} = (\frac{1}{\sqrt{s}}) \sum_{i=1}^{N} E_{Ti} \exp(\pm \eta_i) \ , \tag{2}$$

where N=2 corresponds to a two parton (jet) final state (LO) and N=3 to a three parton (jet) final state (NLO). The pseudorapidity is defined as $\eta = \ln \cot(\theta/2)$, where θ is the polar angle of the outgoing jet with respect to the z-axis. The subscript 1(2) corresponds to a positive (negative) argument in the exponential. The energy scale of the hard scattering, Q^2, is usually defined as $Q^2 = E_T^2$ where E_T is defined as the transverse energy of the jet. Jets are ordered in descending order with respect to E_T, so the "leading jet" refers to the highest E_T jet in the event.

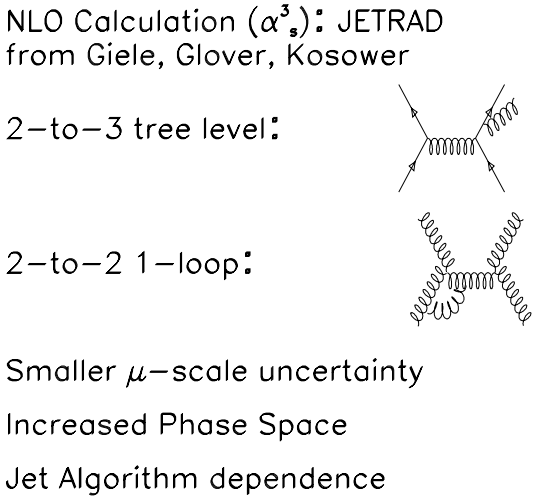

FIGURE 1. Main features of the NLO calculation including the 2-to-3 tree level and 2-to-2 1-loop Feynman diagrams that contribute to the jet production.

Calculations of jet physics are available at NLO (order α_s^3) [2–4]. The NLO theory includes, in addition to the 2-to-2 tree level Feynman diagrams, 2-to-3 tree level and 2-to-2 one-loop diagrams as shown in Fig. 1. The NLO calculation provides a smaller uncertainty due to the renormalization/factorization scale μ [5], and increased phase space in the forward pseudorapidity regions and introduces a jet algorithm dependence. Both experiments use the Snowmass iterative cone algorithm with a cone radius of $\mathcal{R}=\sqrt{(\Delta\eta)^2+(\Delta\phi)^2}=0.7$ in $\eta-\phi$ space [6].

The NLO calculation packages used for the different analyses are EKS and JETRAD [3,4]. The main parameters that can be changed are the PDF's, the μ scale, and the jet cone algorithm. EKS was used with a value of $\mu = E_T^{jet}/2$, where E_T^{jet} is the E_T of the jet while JETRAD was evaluated with $\mu = E_T^{max}/2$, where E_T^{max} is the E_T of the leading jet in the event. At NLO, two partons can be $2R$ apart and still be merged into one jet where R is the jet cone radius. This criterion is used for the jet algorithm used by the CDF collaboration. The DØ collaboration restricts this separation to a value of $R_{SEP} = 1.3$, where R_{SEP} is the value in units of $\mathcal{R}$ of allowed separation [7].

INCLUSIVE JET CROSS SECTION AT $\sqrt{S} = 1800$ GEV

The inclusive jet cross section counts all the jets in the event that satisfy η and E_T criteria. The cross section is written as

$$\frac{d^2\sigma}{dE_T d\eta} = \frac{N}{\Delta E_T \Delta\eta \int \mathcal{L} dt} \tag{3}$$

and plotted as a function of the jet E_T. N is the number of jets in the event, ΔE_T is the E_T bin size, $\Delta\eta$ is the η bin size, and $\int \mathcal{L} dt$ is the integrated luminosity.

The CDF collaboration has measured the jet cross section using the 1992-1993 data sample (run 1A) in the region $0.1 \leq |\eta| \leq 0.7$ and observed an excess above NLO calculations for jet E_T above 200 GeV [1]. The theoretical calculation is made with the EKS algorithm with the renormalization and factorization scales set at $\mu = E_T^{jet}/2$, $R_{sep} = 2.0$ and the CTEQ3M PDF [3,8]. Higher statistics data from the 1994-1995 run (run 1B) continues to exhibit an excess in the jet cross section (Fig. 2).

The DØ collaboration has measured the cross section from run 1B data sample for the regions $0.0 \leq |\eta| \leq 0.5$ and $0.1 \leq |\eta| \leq 0.7$. Figure 3 shows a residual plot for both regions depicting excellent agreement with the NLO theory for the entire E_T range. The theoretical calculation comes from JETRAD with the renormalization and factorization scales set at $\mu = E_T^{max}/2$, $R_{sep} = 1.3$, and the CTEQ3M PDF [4,8].

The data from both experiments for the region $0.1 \leq |\eta| \leq 0.7$ are shown in Fig. 4, in which the DØ data has been compared to a fit of the CDF's published result.

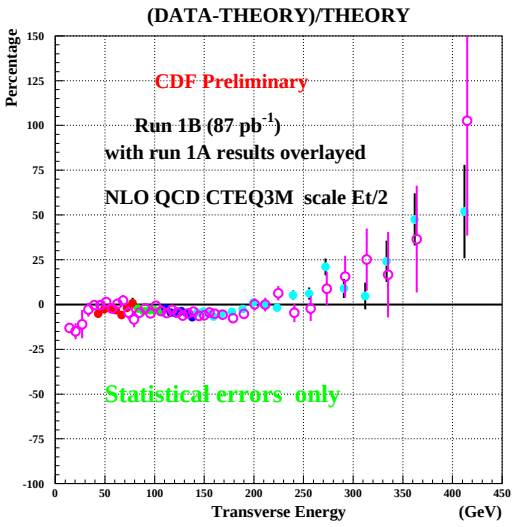

FIGURE 2. Residual plot of the inclusive jet cross section from CDF from run 1B (solid circles) and run 1A (open circles). The theory used was EKS with the CTEQ3M PDF. The error bars are statistical only.

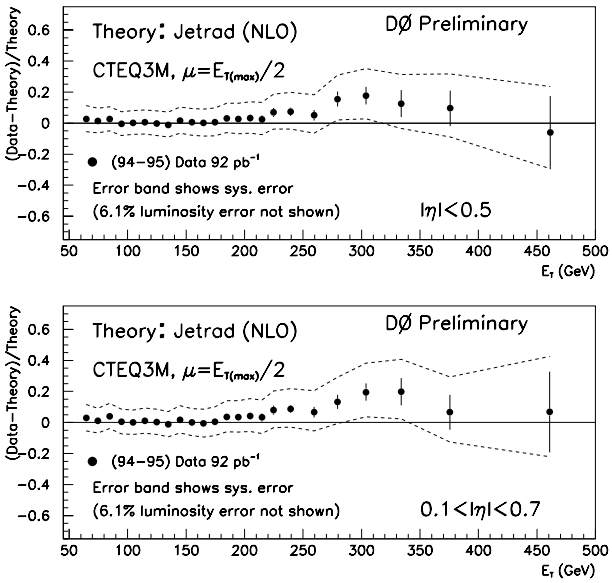

FIGURE 3. Residual plot of the inclusive jet cross section from DØ from run 1B for the regions $0.0 \leq |\eta| \leq 0.5$ (top) and $0.1 \leq |\eta| \leq 0.7$ (bottom). The theory used was JETRAD with the CTEQ3M PDF. The error bars are statistical only. The band shows $\pm$ 1σ systematic uncertainty.

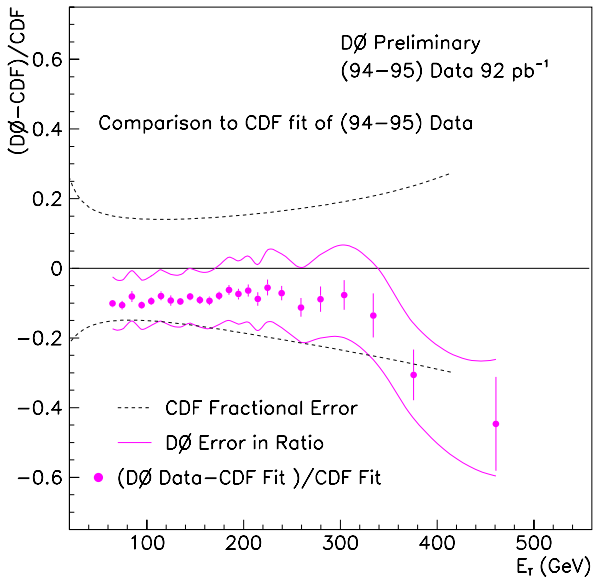

FIGURE 4. Residual plot of the inclusive jet cross section from DØ from run 1B for the region $0.1 \leq |\eta| \leq 0.7$. The reference used was a fit to the CDF's published run 1A data. The error bars are statistical only. Bands correspond to the $\pm$ 1σ systematic uncertainty for each experiment.

INCLUSIVE JET CROSS SECTION AT $\sqrt{S} = 630$ GEV

Both experiments have also measured the inclusive cross section at a lower center-of-mass energy, $\sqrt{s} = 630$ GeV. To allow a direct comparison with the $\sqrt{s} = 1800$ GeV data, the data are plotted as a function of the variable x_T, defined as $x_T = 2E_T/\sqrt{s}$. Figure 5 shows the ratio of the scaled cross sections at $\sqrt{s} = 630$ GeV to that at $\sqrt{s} = 1800$ GeV for both experiments, compared to the same ratio in the theory, as a function of x_T. The experiments are in good agreement with each other but the data lie $15\% - 20\%$ below the theoretical predictions.

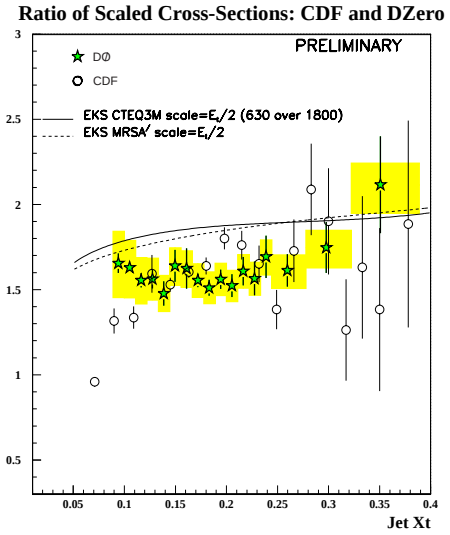

FIGURE 5. The ratio of the scaled cross sections for both CDF (open circles) and DØ (solid stars) with the same ratio from EKS using MRSA′ and CTEQ3M. The error bars are statistical only. The boxes correspond to the $\pm$ 1σ systematic uncertainty for the DØ collaboration.

DIJET ANGULAR DISTRIBUTION

The dijet angular distribution, $\frac{1}{N}\frac{dN}{d\chi}$, is a good tool for determining whether any observed excess of events might be due to compositeness. Compositeness models are extensions to the Standard Model in which quarks are allowed to have substructure. One of the advantages to investigating the angular distribution is that it should be insensitive to the PDF's. One searches for dijet events and plots them as a function of χ, defined as

$$\chi = \exp(|\eta_1 - \eta_2|) = \frac{1 + \cos\theta^*}{1 - \cos\theta^*} \tag{4}$$

for different mass bins, where $\eta_{1,2}$ represents the pseudorapidity of the two leading jets and θ^* represents the center-of-mass scattering angle. The use of χ flattens the angular distribution, facilitating comparison with theory.

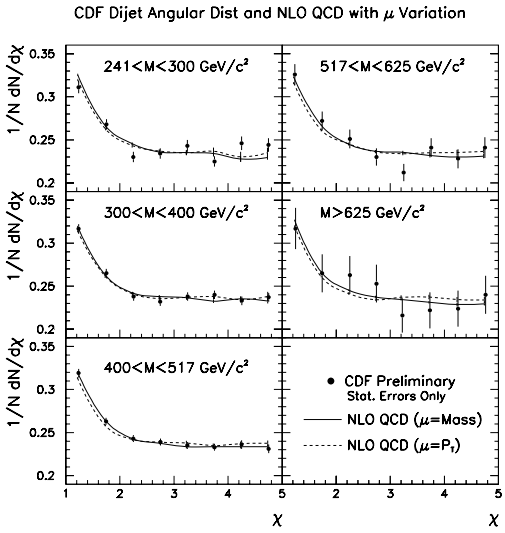

FIGURE 6. Dijet angular distribution as a function of χ (circles) for different mass bins compared to JETRAD for two different μ scales. The error bars are statistical only.

The jets are restricted to $0.1 \leq |\eta_{1,2}| \leq 2.0$ and $\chi < 5$ by the CDF collaboration [9]. Figure 6 compares data with theory and demonstrates that very little variation arises due to the different scales when looking at regions of $\chi < 5$. To determine a limit, a ratio R is defined as

$$R_\chi = \frac{Number\ of\ events\ with\ \chi < 2.5}{Number\ of\ events\ with\ \chi > 2.5} \tag{5}$$

for each mass bin. This procedure removes correlated errors and reduces the curve to a single number. The ratio is then plotted as a function of the mass bin and compared to models with different values of contact terms, which are expressed in the form of the parameters Λ^- and Λ^+ for constructive and destructive interference terms respectively. Fig. 7 shows that the CDF data is in excellent agreement with LO and NLO QCD predictions as well as the behavior of the theoretical predictions for including different contact term values. For a model where all quarks are allowed to be composite objects, the CDF collaboration excludes at the 95% confidence level (CL) regions with $\Lambda^+ \leq 1.8$ TeV and $\Lambda^- \leq 1.6$ TeV.

The DØ search is performed for $0.0 \leq |\eta_{1,2}| \leq 3.0$, which includes χ values up to 20 when kinematically accessible [10]. Though a large range of χ introduces some sensitivity of the theoretical predictions to different renormalization/factorization scales (Fig. 8), the analysis is more sensitive to higher values of Λ. The DØ experiment defines a ratio similar to the CDF collaboration but for different ranges of χ:

$$R_\chi = \frac{Number\ of\ events\ with\ \chi < 4}{Number\ of\ events\ with\ \chi > 4} \tag{6}$$

The DØ experiment rules out a model, in which all quarks are allowed to be composite objects, at the 95% CL regions with $\Lambda^+ \leq 2.0$ TeV.

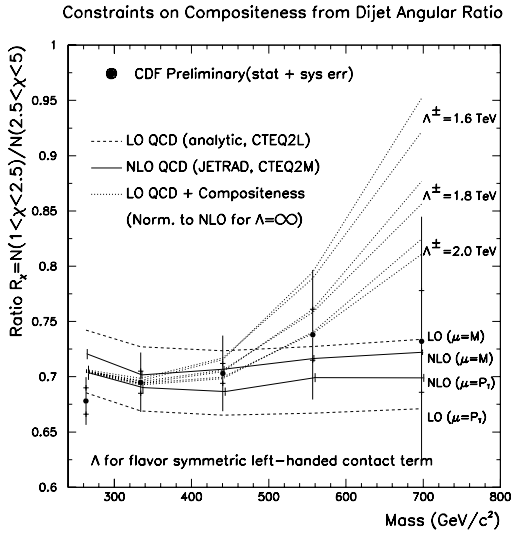

FIGURE 7. The ratio R_χ as a function of mass. The inner error bars are statistical and outer error bars indicate the sum in quadrature of statistical and systematic errors. The data exhibit excellent agreement with LO and NLO QCD. Also shown is the behavior of the theory when different contact term values are included. The higher curve corresponds to destructive interference (Λ^+).

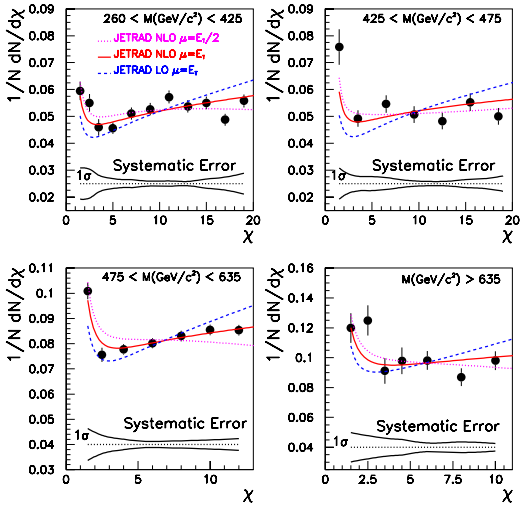

FIGURE 8. Dijet angular distribution for four different mass bins. A wider range of χ allows sensitivity to differences due to the μ scale. The inner error bars are statistical errors only. The band shows $\pm$ 1σ systematic uncertainty.

DIJET INVARIANT MASS

The existence of new particles may be identified by looking for a resonance in their hadronic decay products. The DØ analysis requires the two leading jets to be within $0.0 \leq |\eta| \leq 1.0$ and the CDF analysis requires the two leading jets to be within $0.0 \leq |\eta| \leq 2.0$ and $\cos\theta^* < 2/3$. Figures 9 and 10 show residual plots for both the CDF and DØ analyses respectively. The comparison for CDF is normalized to the first six data points while the DØ comparison is done for absolute normalization. Each result shows very good agreement with JETRAD.

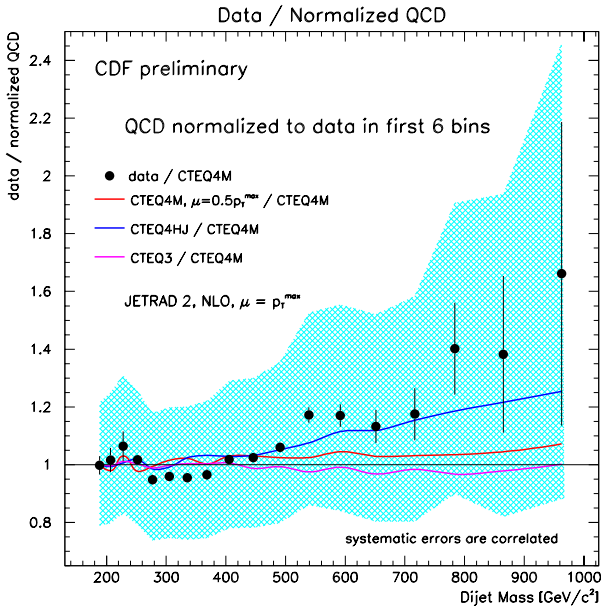

FIGURE 9. The residual plot of the dijet invariant mass with JETRAD with the CTEQ4M PDF where the theory has been normalized to the first six data points. The error bars are statistical only. The boxes show the $\pm$ 1σ systematic uncertainty. Also seen are residual distributions when using other PDF's or μ scales.

To reduce the systematic uncertainty, the DØ collaboration has further subdivided the sample into two η regions, and taken a ratio of the cross sections to reduce the systematic uncertainties ($0.0 \leq |\eta| \leq 0.5$ and $0.5 \leq |\eta| \leq 1.0$). The systematic uncertainty is reduced to $< 10\%$ and still shows good agreement with the theory (Fig. 11).

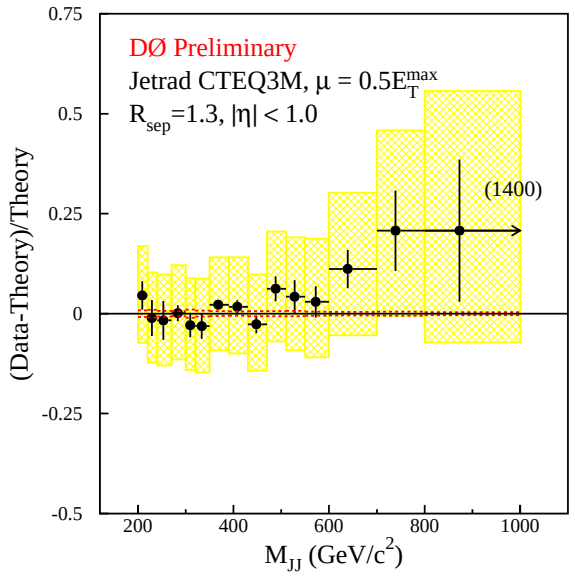

FIGURE 10. The residual plot of the dijet invariant mass with JETRAD with the CTEQ3M PDF. The error bars are statistical only. The band shows the $\pm$ 1σ systematic uncertainty of the theory. The boxes surrounding the data points show the $\pm$ 1σ systematic uncertainty.

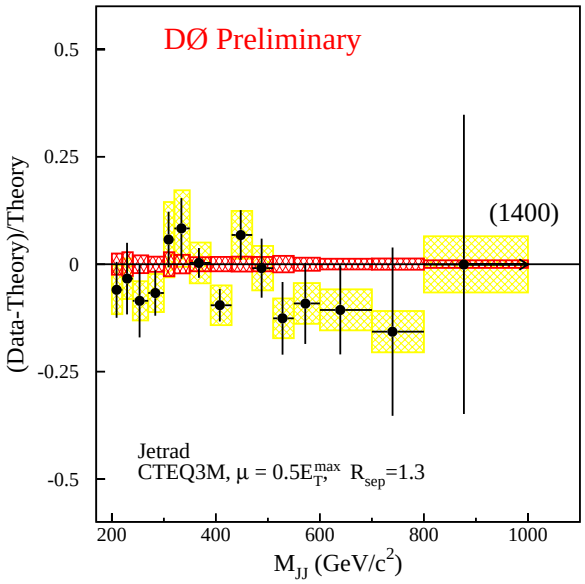

FIGURE 11. The residual plot of the ratio of the two η regions ($0.5 \leq |\eta| \leq 1.0$ over $0.0 \leq |\eta| \leq 0.5$) as a function of the invariant mass with a similar ratio from JETRAD.

TRIPLE DIFFERENTIAL DIJET CROSS SECTION

One explanation for the excess of very high E_T jets observed by the CDF collaboration is the choice of PDF used in the theory Monte Carlo generation. The CTEQ group has found that placing more gluons in the high x region does not strongly affect the fit with other experiments and has released the CTEQ4HJ PDF [11].

The triple differential dijet cross section, $d^3\sigma/dE_T d\eta_1 d\eta_2$ is ideal for the study of different PDF's because the choice of variables are sensitive to the PDF's, while being insensitive to the matrix elements. Hence, the triple differential analysis is complementary to the angular distribution analysis. The CDF collaboration requires the leading jet to be central $(0.1 \leq |\eta_1| \leq 0.7)$ and plots the E_T of the leading jet for four different configurations defined by the position of the second leading jet: $0.1 \leq |\eta_2| \leq 0.7$, $0.7 \leq |\eta_2| \leq 1.4$, $1.4 \leq |\eta_2| \leq 2.1$, and $2.1 \leq |\eta_2| \leq 3.0$ as it is shown in Fig. 12.

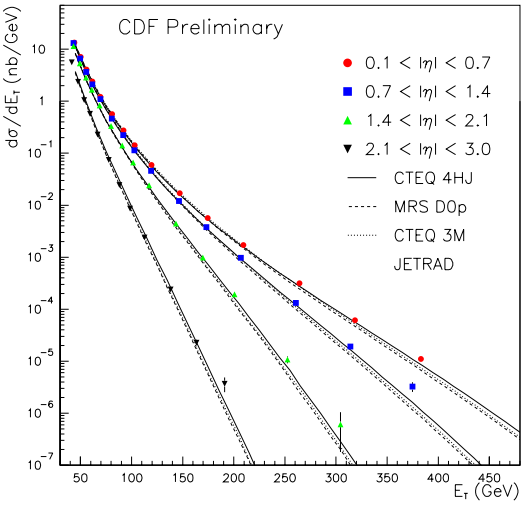

FIGURE 12. The triple differential dijet cross section for the four different η regions compared to JETRAD using different PDF's. The error bars are statistical only.

To linearize the scale, the CDF collaboration weights the cross section by different powers of E_T of the leading jet for the different pseudorapidity regions as shown in Fig. 13. The results in Fig. 13 are not sensitive enough to distinguish among the various PDF's.

CONCLUSIONS AND FUTURE PROSPECTS

A variety of high P_T jet analyses has shown that pQCD is still a very successful theoretical model. There remains a discrepancy in the $\sqrt{s} = 630$ GeV inclusive data where the theory exhibits a $15-20\%$ excess. In the $\sqrt{s} = 1800$ GeV inclusive data sample, the CDF collaboration finds an excess for $E_T > 200$ GeV while the DØ collaboration finds excellent agreement for the entire E_T range. Both experimental data sets are in good agreement for $E_T < 300$ GeV. The CTEQ4HJ PDF remains a possible candidate for

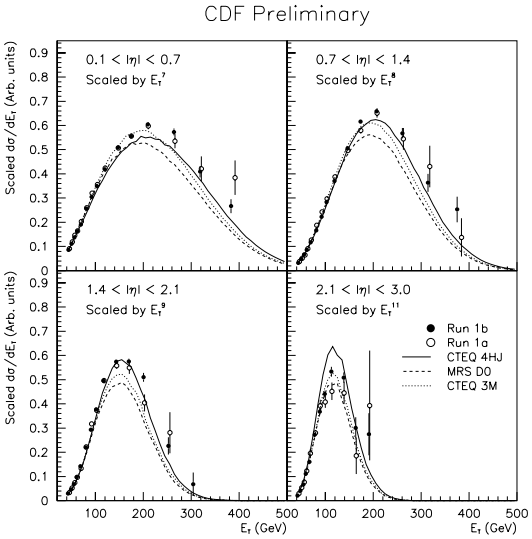

FIGURE 13. The triple differential dijet cross section for the four different η regions scaled by a region-dependent power of E_T compared to JETRAD using various PDF's. The error bars are statistical only.

explaining the excess found by the CDF collaboration. The next Tevatron run, where a factor to 20 in increased luminosity is expected and both detectors will be upgraded, will hopefully produce a definite answer to these remaining questions.

ACKNOWLEDGMENTS

We are grateful to the DØ and CDF collaborations for discussions of their data.

REFERENCES

1. F. Abe *et al.*, (CDF Collaboration), Phys. Rev. Lett. **77**, 428 (1996).
2. F. Aversa *et al.*, Nuclear Physics **B327** (1989).
3. S. Ellis, Z. Kunszt, and D. Soper, Phys. Rev. Lett. **64**,2121 (1990).
4. W. Giele, N. Glover, and D. Kosower, Phys. Rev. Lett. **B73**,2019 (1994).
5. B. Abbott *et al.*, (DØ Collaboration), Hep-Ph/9801285 (1998).
6. J. Huth *et al.*, proceedings of Research Directions for the Decade, Snowmass 1990, pp. 134-136 edited by E. L. Berger (World Scientific, Singapore 1992).
7. B. Abbott *et al.*, (DØ Collaboration), Fermilab-PUB-97/242-E (1997). Phys. Res., Sect. A, **271**, 387 (1988). Phys. Res., Sect. A, **338**, 185 (1994).
8. H. Lai *et al.*, (CTEQ Collaboration), Phys. Rev. **D51**, 4763 (1995).
9. F. Abe *et al.*, (CDF Collaboration), Phys. Rev. Lett. **78**, 4397 (1997).
10. B. Abbott *et al.*, (DØ Collaboration), Phys. Rev. Lett. **80**, 666 (1998).
11. H. Lai *et al.*, (CTEQ Collaboration), Phys. Rev. **D55**, 1280 (1997).